Results in Physics 8 (2018) 34–40

Contents lists available at ScienceDirect

Results in Physics

journal homepage: www.journals.elsevier.com/results-in-physics

Simulation of ferromagnetic nanomaterial flow of Maxwell fluid

T. Hayat [a,b], Salman Ahmad [a], M. Ijaz Khan [a,*], A. Alsaedi [b]

[a] Department of Mathematics, Quaid-I-Azam University, 45320 Islamabad 44000, Pakistan
[b] Nonlinear Analysis and Applied Mathematics (NAAM) Research Group, Department of Mathematics, Faculty of Science, King Abdulaziz University, P.O. Box 80257, Jeddah 21589, Saudi Arabia

ARTICLE INFO

Article history:
Received 27 October 2017
Accepted 15 November 2017
Available online 24 November 2017

Keywords:
Rate type fluid
Brownian movement
Thermophoresis effect
Magnetic dipole

ABSTRACT

Ferromagnetic flow of rate type liquid over a stretched surface is addressed in this article. Heat and mass transport are investigated with Brownian movement and thermophoresis effects. Magnetic dipole is also taken into consideration. Procedure of similarity transformation is employed. The obtained nonlinear expressions have been tackled numerically by means of Shooting method. Graphical results are shown and analyzed for the impact of different variables. Temperature and concentration gradients are numerically computed in Tables 1 and 2. The results described here demonstrate that ferromagnetic variable boosts the thermal field. It is noticed that velocity and concentration profiles are higher when elastic and thermophoresis variables are enhanced.

Introduction

Ferrofluids are the suspension of nanoscale ferromagnetic particles in fluid carrier and magnetized by the influence of magnetic field. It is artificially synthesized and have various application. Ferrofluids are used in different equipment like laser, heat treating furnaces, avionics, cooling agent, nuclear power plants, X-ray machine, semiconductor processing, fiber optics, crystal processing, textiles machine tools, robotics, loudspeakers, refrigeration, filtration, drawing plastic, metal spinning and computer peripherals etc. On the basis of these uncountable importance many scientists and researchers accelerate the study of ferrofluids. Thermophysical characteristics of ferrohydrodynamics are examined by Neuringer and Rosensweig [1]. Anderson and valnes [2] explored effect of magnetic dipole and heat transfer in flow of ferrofluid over a stretchable surface. Yasmeen et al. [3] and Hayat et al. [4] discussed characteristics of ferrofluids with mixed convection, homogeneous-heterogenous reactions and magnetic dipole. The impacts of suction/injection and magnetic dipole in flow of viscoelastic material is studied by Zeeshan and Majeed [5]. Sheikholeslami et al. [6] elaborated effects of non-uniform magnetic field in magnetic iron oxide water nanomaterial. Zeeshan et al. [7] examined simultaneous impacts of magnetic dipole and radiation in flow of viscous ferrofluid. Magnetic and thermodynamic characteristics of ferrofluids through influence of external magnetic field is investigated by Vtulkina and Elfimova [8]. Some studies exploring ferrofluid concept and heat and mass transfer analysis can be seen in Refs. [9–13].

It is recognized now that all non-Newtonian materials in view of their diverse characteristics are not examined by one constitutive relation. Thus non-Newtonian materials are classified for differential, rate and integral types [14–25]. Some examples of non-Newtonian materials include synovial fluids, gypsum paste, printer ink, yogurt, clays, hydrogenated caster oil, drilling mud, paints, colloidal suspension, blood, toothpaste taffy, mayonnaise, butter, cheese, ketchup, soup, jam, shampoos etc. In present attempt we consider Maxwell fluid model (a subclass of rate type fluid model). Studies associated with Maxwell fluid are presented through Refs. [26–29].

In this attempt we explore the effect of magnetic dipole in flow of rate type ferroliquid over a stretchable sheet. Brownian motion and thermophoresis diffusion are also accounted. Suitable transformation is applied to obtain the nonlinear system. For numerical solution we adopt shooting technique [30–35]. Effects of involved parameters on temperature, velocity and concentration are discussed. Temperature and mass gradients are also explored numerically.

Problem description

Here ferromagnetic flow of an incompressible rate type nanomaterial with Brownian motion and thermophoresis is considered. The constitutive relations for Maxwell fluid are employed. An

* Corresponding author.
E-mail address: mikhan@math.qau.edu.pk (M.I. Khan).

https://doi.org/10.1016/j.rinp.2017.11.021
2211-3797/

incompressible fluid over a stretching surface is discussed. Temperature and concentration of ferroliquid at sheet are T_w and C_w respectively while $T \to T_c$ and $C \to C_c$ at $y \to \infty$ are ambient temperature and concentration. Geometrical configuration of relevant flow is displayed in Fig. 1. The relevant equations in view of standard boundary layer assumption are:

$$\frac{\partial u}{\partial x}+\frac{\partial v}{\partial y}=0, \tag{1}$$

$$u\frac{\partial u}{\partial x}+v\frac{\partial u}{\partial y}=\nu\frac{\partial^2 u}{\partial y^2}+\frac{\mu_0 M}{\rho}\frac{\partial H}{\partial x} + \lambda\left\{u^2\frac{\partial^2 u}{\partial x^2}+v^2\frac{\partial^2 u}{\partial y^2}+2uv\frac{\partial^2 u}{\partial x\partial y}\right\}, \tag{2}$$

$$u\frac{\partial T}{\partial x}+v\frac{\partial T}{\partial y}+\mu_0 T\frac{\partial M}{\partial T}\left(u\frac{\partial H}{\partial x}+v\frac{\partial H}{\partial y}\right) = \frac{k}{\rho c_p}\frac{\partial^2 T}{\partial y^2}+\tau\left\{D_B\left(\frac{\partial C}{\partial y}\frac{\partial T}{\partial y}\right)+\frac{D_T}{T_c}\left(\frac{\partial T}{\partial y}\right)^2\right\}, \tag{3}$$

$$u\frac{\partial C}{\partial x}+v\frac{\partial C}{\partial y}=D_B\frac{\partial^2 C}{\partial y^2}+\frac{D_T}{T_c}\frac{\partial^2 T}{\partial y^2}, \tag{4}$$

with

$$u(0)=cx,\quad v(0)=0,\quad T(0)=T_w,\quad C(0)=C_w,\quad u|_{y\to\infty}\to 0, \quad T|_{y\to\infty}\to T_c,\quad C|_{y\to\infty}\to C_c, \tag{5}$$

in which u and v represent velocities in x and y directions, ν dynamic viscosity, μ_0 magnetic permeability, M magnetization, ρ density of fluid, H magnetic field, λ relaxation time, T fluid temperature, k thermal conductivity, c_p specific heat, D_B Brownian diffusion coefficient, D_T thermal diffusion coefficient and C concentration.

Expression of scalar magnetic potential is

$$\Phi=\frac{\gamma}{2\pi}\frac{x}{x^2+(y+a)^2}, \tag{6}$$

where a represents the distance between origin and center of magnetic dipole and γ strength of magnetic field. In components form the scaler magnetic potential are

$$H_x=-\frac{\partial\Phi}{\partial x}=\frac{\gamma}{2\pi}\frac{x^2-(y+a)^2}{\left[x^2+(y+a)^2\right]^2}, \tag{7}$$

$$H_y=-\frac{\partial\Phi}{\partial y}=\frac{\gamma}{2\pi}\frac{2x(y+a)}{\left[x^2+(y+a)^2\right]^2}. \tag{8}$$

The magnitude of magnetic field **H** is

$$H=\left\{\left(\frac{\partial\Phi}{\partial x}\right)^2+\left(\frac{\partial\Phi}{\partial y}\right)^2\right\}^{\frac{1}{2}}. \tag{9}$$

From Eqs. (9) and (10) one can write

$$\frac{\partial H}{\partial x}=-\frac{\gamma}{2\pi}\frac{2x}{(y+a)^4}, \tag{10}$$

$$\frac{\partial H}{\partial y}=\frac{\gamma}{2\pi}\left\{-\frac{2}{(y+a)^3}+\frac{4x^2}{(y+a)^5}\right\}. \tag{11}$$

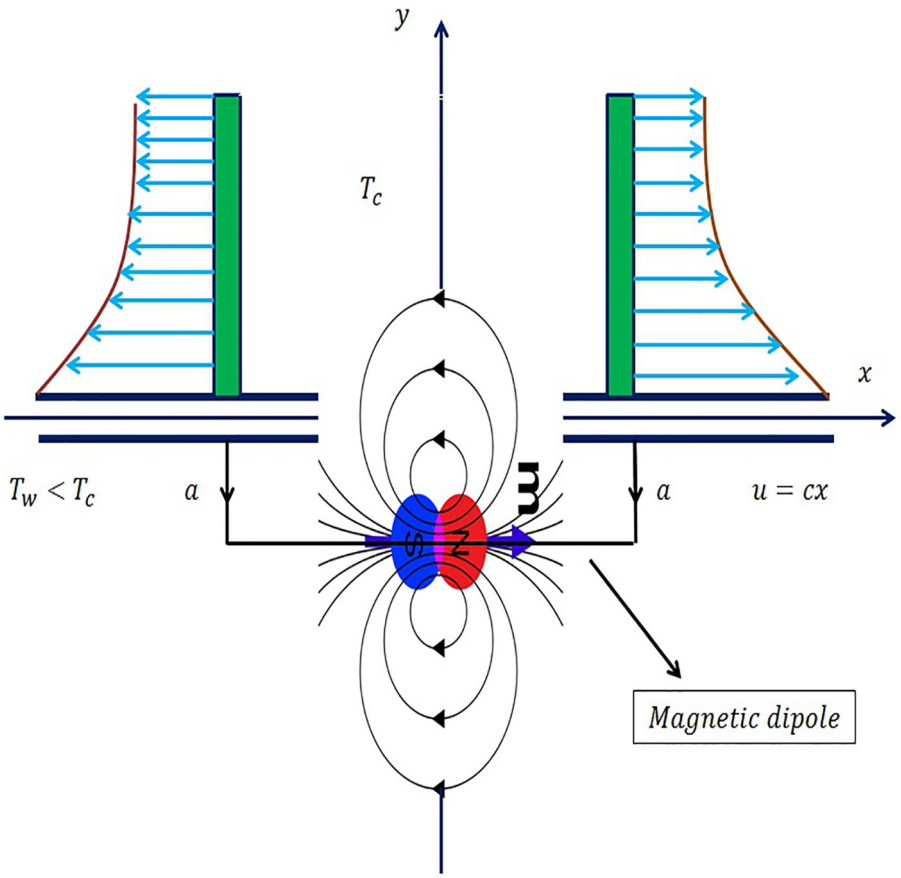

Fig. 1. Flow geometry.

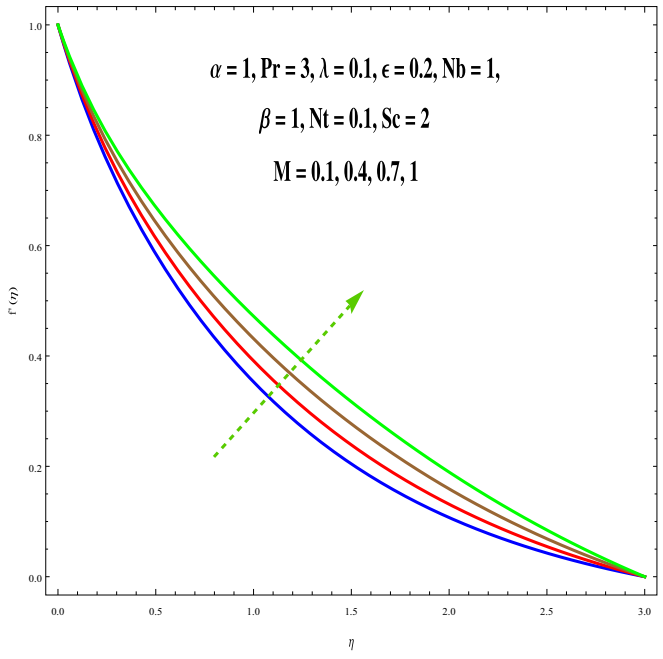

Fig. 2. M variation on $f'(\eta)$.

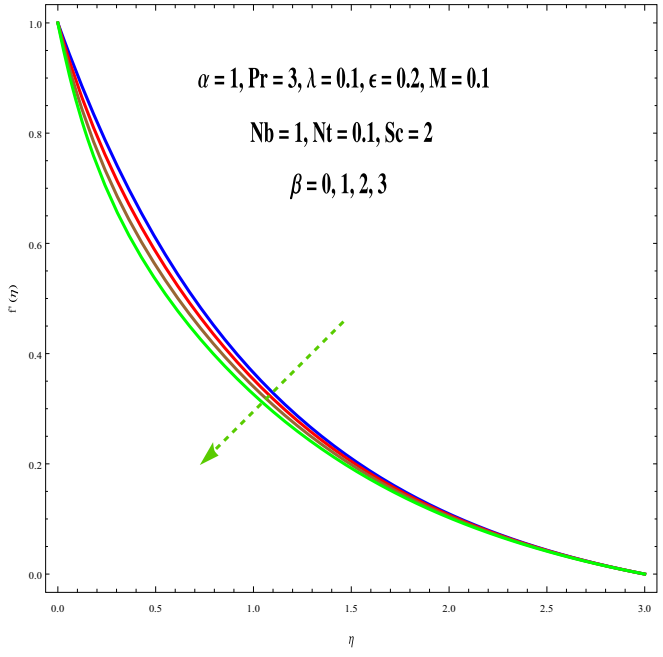

Fig. 3. β variation on $f'(\eta)$.

Magnetization M through temperature T can be approximated as

$$M = K(T_c - T), \tag{12}$$

where K shows gyromagnetic coefficient constant.

Solution procedure

Adopting appropriate transformation

$$\psi(\xi,\eta) = \frac{\mu}{\rho}\xi f(\eta), \quad \theta(\eta) = \frac{T_c - T}{T_c - T_w}, \quad \phi(\eta) = \frac{C_c - C}{C_c - C_w}, \quad \eta = \sqrt{\frac{c\rho}{\mu}}y,$$
$$\xi = \sqrt{\frac{c\rho}{\mu}}y, \quad u = \frac{\partial\psi}{\partial y} = cxf'(\eta), \quad v = -\frac{\partial\psi}{\partial x} = -\sqrt{\frac{c\mu}{\rho}}f(\eta), \tag{13}$$

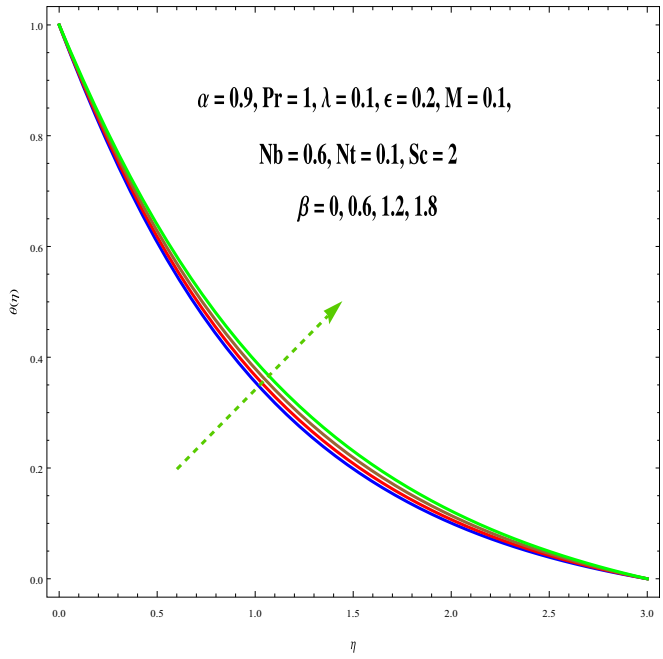

Fig. 4. β variation on $\theta(\eta)$.

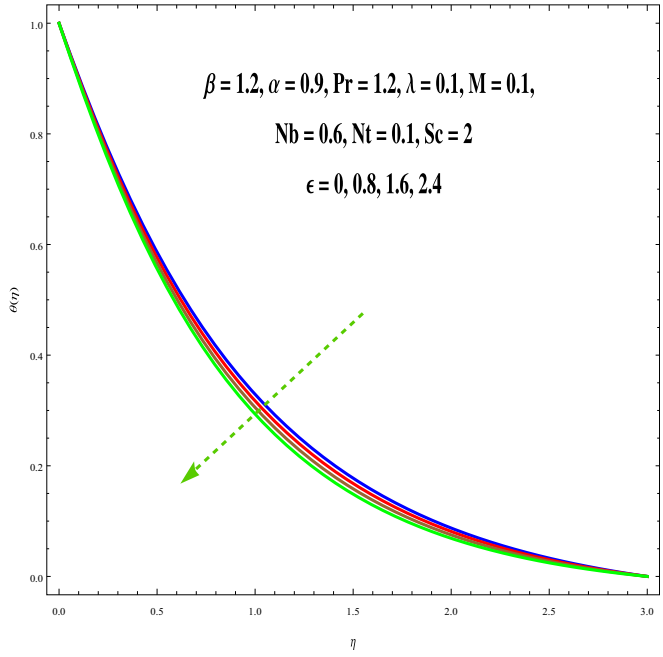

Fig. 5. ϵ variation on $\theta(\eta)$.

we have

$$f''' + ff'' - (f')^2 + M(f^2 f''' - 2ff'f'') - \frac{2\beta\theta}{(\eta+\alpha)^4} = 0 \tag{14}$$

$$\theta'' + Pr(f\theta' - Nb\theta'\phi' - Nt(\phi')^2) + \frac{2\lambda\beta(\theta-\epsilon)f}{(\eta+\alpha)^3} = 0 \tag{15}$$

$$\phi'' + Sc\left(f\phi' + \frac{Nt}{Nb}\theta''\right) = 0 \tag{16}$$

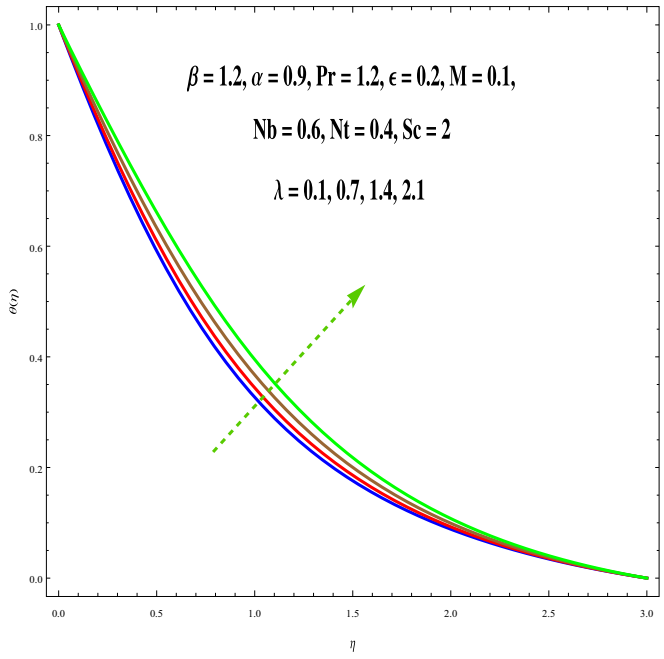

Fig. 6. λ variation on $\theta(\eta)$.

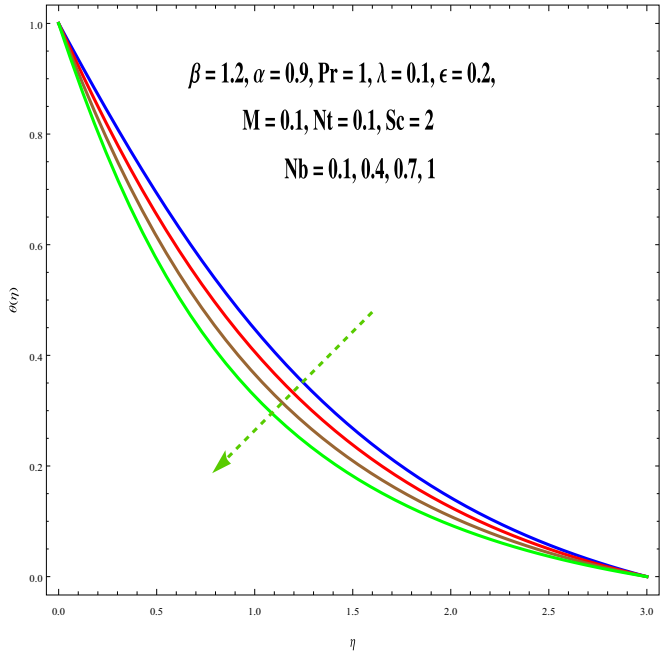

Fig. 7. *Nb* variation on $\theta(\eta)$.

$$f(0)=0,\quad f'(0)=1,\quad \theta(0)=1,\quad \phi(0)=1,\quad f'|_{\eta\to\infty}\to 0,$$
$$\theta|_{\eta\to\infty}\to 0,\quad \phi|_{\eta\to\infty}\to 0, \tag{17}$$

where M indicates elastic parameter, β ferrohydrodynamic interaction, α dimensionless distance, Pr Prantal number, Nb Brownian motion, Nt thermophoresis, λ Eckert number, ϵ dimensionless temperature and Sc Schmidt number. These definitions are

$$M=\lambda c,\quad \beta=\frac{\gamma\rho\mu_0}{2\pi\mu^2}K(T_c-T_w),\quad \alpha=a\sqrt{\frac{c\rho}{\mu}},\quad Pr=\frac{\mu c_p}{k},$$
$$Nb=\frac{\tau D_B(C_c-C_w)}{v},Nt=\frac{\tau D_T(T_c-T_w)}{T_c v},\quad \lambda=\frac{c\mu^2}{\rho k(T_c-T_w)},$$
$$\epsilon=\frac{T_c}{T_c-T_w},\quad Sc=\frac{v}{D_B}. \tag{18}$$

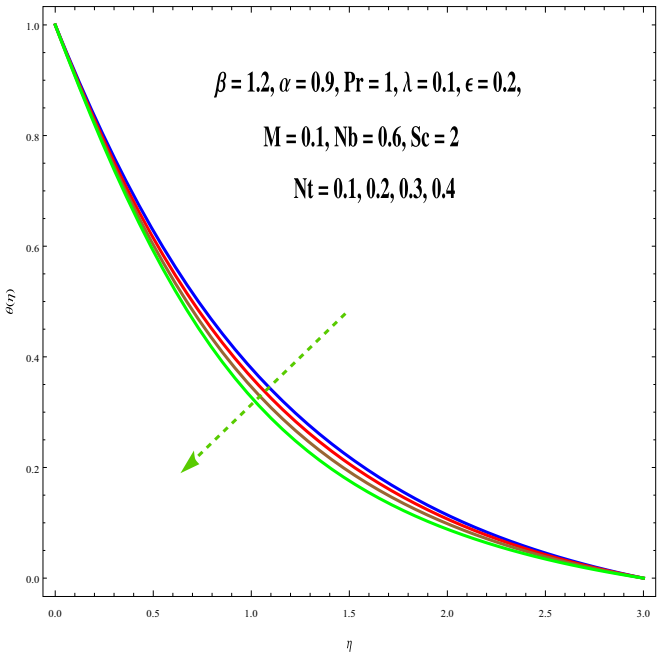

Fig. 8. *Nt* variation on $\theta(\eta)$.

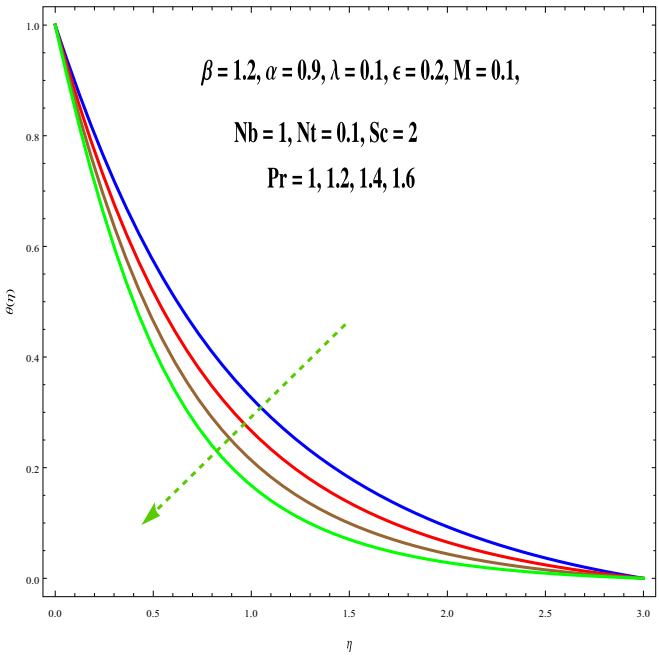

Fig. 9. *Pr* variation on $\theta(\eta)$.

Mathematical expressions for local Nusselt and Sherwood numbers are

$$Nu_x=\frac{xq_w}{k(T_c-T_w)},\quad Sh_x=\frac{xq_m}{D_B(C_c-C_w)}, \tag{19}$$

where

$$q_w=-k\left(\frac{\partial T}{\partial y}\right)_{y=0},\quad q_m=-D_B\left(\frac{\partial C}{\partial y}\right)_{y=0}. \tag{20}$$

Invoking Eq. (20) in Eq. (19) we get

$$Nu_x=-\theta'(0)(Re_x)^{\frac{1}{2}},\quad Sh_x=-\phi'(0)(Re_x)^{\frac{1}{2}}, \tag{21}$$

where $Re_x=\frac{\alpha^2}{v}$ denotes the local Reynolds number.

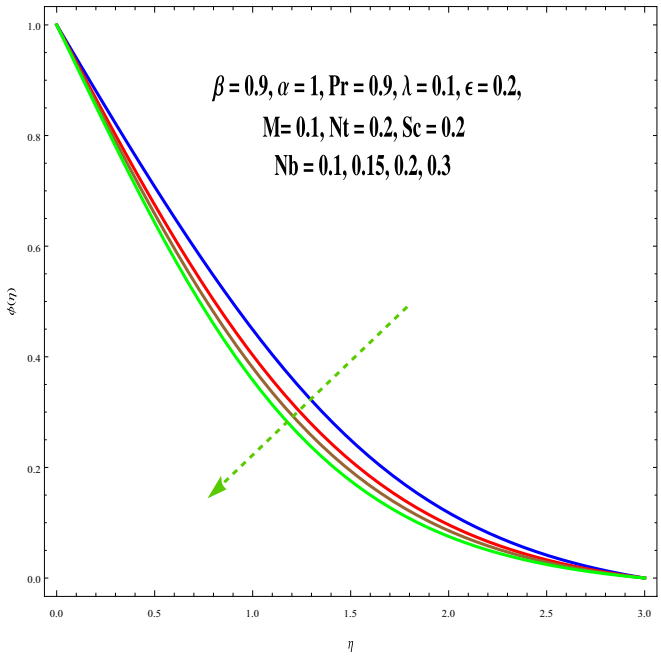

Fig. 10. *Nb* variation on $\phi(\eta)$.

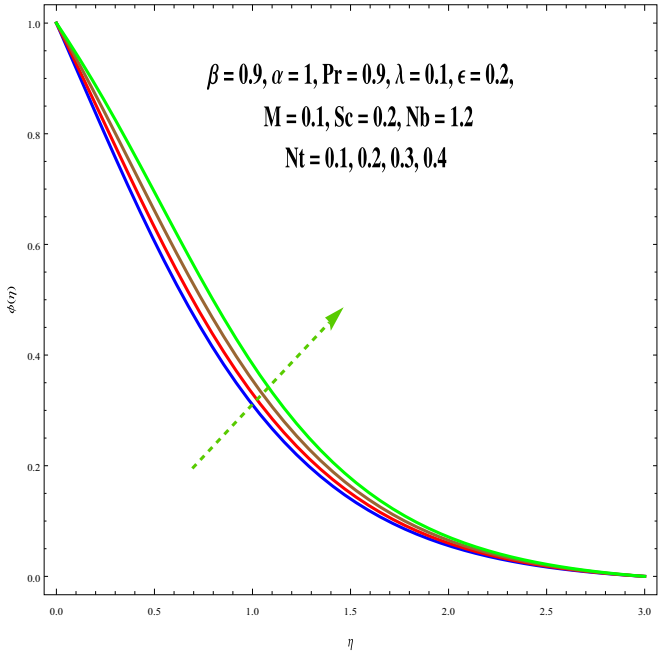

Fig. 11. *Nt* variation on $\phi(\eta)$.

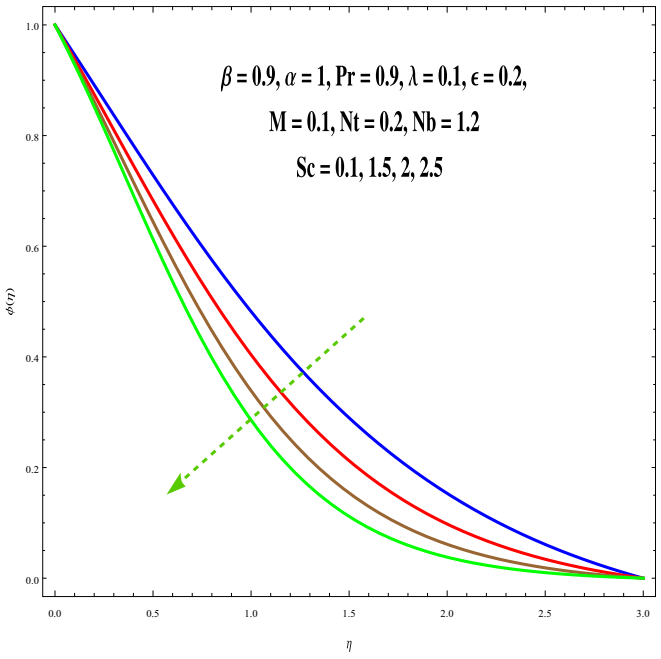

Fig. 12. *Sc* variation on $\phi(\eta)$.

Outcomes and discussion

Numerical technique namely (Built-in-Shooting) utilized here leads to computational results of resulting differential systems. The effects of sundry variables like elastic parameter (M), ferrohydrodynamic interaction (β), Prantal number (Pr), Brownian parameter (Nb), thermophoresis variable (Nt), Eckert number (λ), dimensionless temperature (ϵ) and Schmidt number (Sc) on temperature $(\theta(\eta))$, concentration $(\phi(\eta))$ and velocity $(f'(\eta))$ are portrayed in Figs. 2–12.

Fig. 2 illustrates effect of elastic parameter (M) on $f'(\eta)$. Here velocity is retarded for larger estimation of elastic parameter (M). Clearly elastic variables involve relaxation time. Fluids with smaller elastic variable behave like a liquid while for larger M these behave like solid materials. Liquid viscosity increases for higher (M) which gives more resistive force to fluid flow and as a result velocity decays. Fig. 3 depicts velocity curves against ferromagnetic interaction variable (β). Here $f'(\eta)$ decays for larger (β). Physically larger values of β provides more resistance to fluid flow. Therefore $f'(\eta)$ decreases.

Figs. 4–9 are plotted to analyze the effects of (β), $(\epsilon), (\lambda), (Nb), (Nt)$ and (Pr) on temperature $(\theta(\eta))$. Fig. 4 presents that increasing values of ferromagnetic interaction variables correspond to higher temperature field. Physically for larger (β) resistive force (Lorentz force) enhances and thus $(\theta(\eta))$ increases. Fig. 5 depicts the change in $(\theta(\eta))$ for different estimation of curie temperature variable (ϵ). An increase in (ϵ) leads to lower thermal field $(\theta(\eta))$. Fig. 6 shows influence of viscous dissipation (Eckert number) on $(\theta(\eta))$. With the increase in (λ) temperature field enhances near the surface. Physically for higher estimation of (λ) internal energy of liquid increases and thus temperature field enhances. Effects of Brownian motion (Nb) and thermophoresis (Nt) parameters on temperature field $(\theta(\eta))$ are sketched in Figs. 7 and 8. From these Figs., we noticed that $(\theta(\eta))$ is reduced for both larger estimation of (Nb) and (Nt). Fig. 9 displays that larger estimation of (Pr) correspond to lower temperature $(\theta(\eta))$. In fact larger (Pr) correspond to higher momentum diffusion and thinner thermal layer. Ultimate the values of $\theta(\eta)$ decay.

Figs. 10–12 eximine behavior of concentration against Nb, Nt and Sc. Effect of Nb on $\phi(\eta)$ is explored in Fig. 11. Concentration is reduced by increasing Brownian parameter (Nb). Physically (Nb) enhances Brownian diffusion rate and as a result concentration reduces. From Fig. 11 we conclude that concentration increases by thermophoresis parameter (Nt). Concentration is found to increase for larger Nt. Behavior of (Sc) on $\phi(\eta)$ is shown in Fig. 12. Here $\phi(\eta)$ is decreasing function of (Sc). Physically Sc enhances momentum diffusivity and thus $(\phi(\eta))$ decreases.

Table 1 communicates the computational results of temperature gradient (Nusselt number) against certain physical variables. Here Table 2 heat transfer rate enhances for larger Nb, Sc, β and M, while it decays for $\alpha, \lambda, \epsilon$ and Nb. Table 2 gives results of

Table 1
Numerical values for Nu_x.

β	α	Pr	ϵ	λ	Nt	Nb	Sc	M	$-\theta'(0)(Re)^{-\frac{1}{2}}$
0.1	0.4	0.8	0.1	0.3	0.2	0.1	0.2	0.5	0.590619
0.2									0.549361
0.3									0.508338
	0.5								0.606693
	0.6								0.615190
	0.7								0.620168
		0.9							0.626713
		1.0							0.662634
		1.1							0.698277
			0.2						0.593601
			0.3						0.596583
			0.4						0.599564
				0.4					0.584574
				0.5					0.578504
				0.6					0.572408
					0.3				0.604659
					0.4				0.617791
					0.5				0.629937
						0.2			0.610401
						0.3			0.630150
						0.4			0.650127
							0.5		0.590619
							0.6		0.593736
							0.7		0.596869
								0.3	0.592435
								0.4	0.594294
								0.5	0.596190

Table 2
Numerical values for Sh_x.

β	α	Pr	ϵ	λ	Nt	Nb	Sc	M	$-\phi'(0)(Re)^{-\frac{1}{2}}$
0.1	0.4	0.8	0.1	0.3	0.2	0.1	0.2	0.5	0.367060
0.2									0.366196
0.3									0.364071
	0.5								0.367324
	0.6								0.367305
	0.7								0.367225
		0.9							0.361208
		1.0							0.354539
		1.1							0.347049
			0.2						0.366727
			0.3						0.366385
			0.4						0.366034
				0.4					0.367604
				0.5					0.368104
				0.6					0.368560
					0.3				0.353874
					0.4				0.338596
					0.5				0.321274
						0.2			0.375905
						0.3			0.378787
						0.4			0.380167
							0.5		0.367060
							0.6		0.367352
							0.7		0.367644
								0.3	0.384441
								0.4	0.402070
								0.5	0.419877

Sherwood number against different physical variable. Here mass transfer rate enhances for increasing the values of $(\beta), (\alpha), (Pr)$ and (ϵ), whiled decreases for (λ) and (Nt).

Conclusion

Effect of magnetic dipole in flow of Maxwell liquid is studied. Main observations here include:

- Velocity is increasing function of elastic parameter (M) while it decays for ferromagnetic parameter (β).
- Temperature enhances by β, λ and it decays through ϵ, Pr.
- Concentration boosts via Nt and Sc and it degrades with Nb.
- Influences of Pr and β on heat transfer rate are different.
- Outcomes of Nt on Sherwood number is opposite to that of Nb and Sc.

Acknowledgments

We are grateful to Higher Education Commission (HEC) of Pakistan for financial support of this work under the project No. 20-3038/NRPU/R & D/HEC/13.

References

[1] Neuringer JL, Rosensweig RE. Ferrohydrodynamics. Phys Fluids 1964;7:1927–37.
[2] Andersson HI, Valnes OA. Flow of a heated ferrofluid over a stretching sheet in the presence of a magnetic dipole. Acta Mech 1998;128:39–47.
[3] Yasmeen T, Hayat T, Khan MI, Imtiaz M, Alsaedi A. Ferrofluid flow by a stretched surface in the presence of magnetic dipole and homogeneous-heterogeneous reactions. J Mol Liq 2016;223:1000–5.
[4] Hayat T, Khan MI, Imtiaz M, Alseadi A, Waqas M. Similarity transformation approach for ferromagnetic mixed convection flow in the presence of chemically reactive magnetic dipole. AIP Phys Fluids 2016;28:102003.
[5] Zeshan A, Majeed A. Heat transfer analysis of Jeffery fluid flow over a stretching sheet with suction/injection and magnetic dipole effect. Alex Eng J 2016;55:2171–81.
[6] Sheikholeslami M, Rashidi MM, Ganji DD. Effect of non-uniform magnetic field on free convection of FeO water nanofluid. Comput Methods Appl Mech Eng 2015;294:299–312.
[7] Zeeshan A, Majeed A, Ellahi R. Effect of magnetic dipole on viscous ferro-fluid past a stretching surface with thermal radiation. J Mol Liq 2016;215:549–54.
[8] Vtulkina ED, Elfimova EA. Thermodynamic and magnetic properties of ferrofluids in external uniform magnetic field. J Magn Magn Mater 2017;431:218–21.
[9] Kamali S, Pouryazdan M, Ghafari M, Itou M, Rahman M, Stroeve P, et al. Magnetization and stability study of a cobalt-ferrite-based ferrofluid. J Magn Magn Mater 2016;404(15):143–7.
[10] Aursand E, Gjennestad MA, Lervåg KY, Lund H. A multi-phase ferrofluid flow model with equation of state for thermomagnetic pumping and heat transfer. J Magn Magn Mater 2016;402:8–19.
[11] Mojumder S, Rabbi KM, Saha S, Hasan M, Saha SC. Magnetic field effect on natural convection and entropy generation in a half-moon shaped cavity with semi-circular bottom heater having different ferrofluid inside. J Magn Magn Mater 2016;407:412–24.
[12] Qasim M, Khan ZH, Khan WA, Shah IA. MHD boundary layer slip flow and heat transfer of ferrofluid along a stretching cylinder with prescribed heat flux. PLoS One 2014;9:e83930.
[13] Mustafa I, Javed T, Ghaffari A. Heat transfer in MHD stagnation point flow of a ferrofluid over a stretchable rotating disk. J Mol Liq 2016;219:526–32.
[14] Hayat T, Sajid M. On analytic solution for thin film flow of a fourth grade fluid down a vertical cylinder. Phys Lett A 2004;361:316–22.
[15] Ibrahim W, Makinde OD. The effect of double stratification on boundary-layer flow and heat transfer of nanofluid over a vertical plate. Comput Fluid 2013;86:433–41.
[16] Ahmad L, Khan M, Khan WA. Numerical investigation of magneto-nanoparticles for unsteady 3D generalized Newtonian liquid flow. Eur Phys J Plus 2017;132:373. 132.
[17] Ayub M, Rasheed A, Hayat T. Exact flow of a third grade fluid past a porous plate using homotopy analysis method. Int J Eng Sci 2003;41:2091–103.
[18] Sheikholeslami M, Ganji DD, Rashidi MM. Ferrofluid flow and heat transfer in a semi annulus enclosure in the presence of magnetic source considering thermal radiation. J Taiwan Inst Chem Eng 2015;47:6–17.
[19] Hayat T, Ahmad S, Khan MI, Alsaedi A. Non-Darcy Forchheimer flow of ferromagnetic second grade fluid. Results Phys 2017;7:3419–24.
[20] Waqas M, Farooq M, Khan MI, Alsaedi A, Hayat T, Yasmeen T. Magnetohydrodynamic (MHD) mixed convection flow of micropolar liquid due to nonlinear stretched sheet with convective condition. Int J Heat Mass Transfer 2016;102:766–72.
[21] Hayat T, Khan MI, Farooq M, Alsaedi A, Waqas M, Yasmeen T. Impact of Cattaneo-Christov heat flux model in flow of variable thermal conductivity fluid over a variable thicked surface. Int J Heat Mass Transfer 2016;99:702–10.
[22] Hayat T, Khan MI, Farooq M, Yasmeen T, Alsaedi A. Stagnation point flow with Cattaneo-Christov heat flux and homogeneous-heterogeneous reactions. J Mol Liq 2016;220:49–55.
[23] Farooq M, Khan MI, Waqas M, Hayat T, Alsaedi A, Khan MI. MHD stagnation point flow of viscoelastic nanofluid with non-linear radiation effects. J Mol Liq 2016;221:1097–103.
[24] Khan MI, Waqas M, Hayat T, Alsaedi A. A comparative study of Casson fluid with homogeneous-heterogeneous reactions. J Colloid Interface Sci 2017;498:85–90.
[25] Qayyum S, Khan MI, Hayat T, Alsaedi A. A framework for nonlinear thermal radiation and homogeneous-heterogeneous reactions flow based on silver-water and copper-water nanoparticles: a numerical model for probable error. Results Phys 2016;7:1907–14.
[26] Khan MI, Waqas M, Hayat T, Khan MI, Alsaedi A. Behavior of stratification phenomenon in flow of Maxwell nanomaterial with motile gyrotactic microorganisms in the presence of magnetic field. IntJ Mech Sci 2017;131–132:426–34.
[27] Zheng L, Zhao F, Zhang X. Exact solutions for generalized Maxwell fluid flow due to oscillatory and constantly accelerating plate. Nonlinear Anal Real World Appl 2010;11:3744–51.
[28] Khan MI, Khan MI, Waqas M, Hayat T, Alsaedi A. Chemically reactive flow of Maxwell liquid due to variable thicked surface. Int Commun Heat Mass Transfer 2017;86:231–8.
[29] Abbas Z, Sajid M, Hayat T. MHD boundary-layer flow of an upper-convected Maxwell fluid in a porous channel. Theor Comput Fluid Dyn 2006;20:229–38.
[30] Hayat T, Khan MI, Qayyum S, Alsaedi A. Modern developments about statistical decleration and probable error for skin fraction and nusselt number with copper and silver nanoparticles. Chin J Phys (in press).
[31] Hayat T, Khan MI, Tamoor M, Waqas M, Alsaedi A. Numerical simulation of heat transfer in MHD stagnation point flow of Cross fluid model towards a stretched surface. Results Phys 2017;7:1824–7.
[32] Waqas M, Khan MI, Hayat T, Alsaedi A. Numerical simulation for magneto Carreau nanofluid model with thermal radiation: a revised model. Comput Methods Appl Mech Eng 2017;324:640–53.
[33] Hayat T, Khan MI, Alsaedi A, Waqas M. Mechanism of chemical aspect in ferromagnetic flow of second grade liquid. Results Phys 2017;7:4162–7.
[34] Hayat T, Khan MI, Alsaedi A, Khan MI. Joule heating and viscous dissipation in flow of nanomaterial by a rotating disk. Int Commun Heat Mass Transfer 2017;89:190–7.
[35] Waqas M, Khan MI, Hayat T, Alsaedi A, Khan MI. Nonlinear thermal radiation in flow induced by a slendering surface accounting thermophoresis and Brownian diffusion. Eur Phys J Plus 2017;132:280. 132.